Biogeosciences
Discussions

Open Access

Evaluating the Community Land Model in a pine stand with $^{13}CO_2$ labeling and shading manipulations

J. Mao, D. M. Ricciuto, P. E. Thornton, J. M. Warren, A. W. King, X. Shi, C. M. Iversen, and R. J. Norby

Evironmental Sciences Division and Climate Change Science Institute, Oak Ridge National Laboratory, Oak Ridge, Tennessee, USA

Correspondence to: J. Mao (maoj@ornl.gov)

BGD

12, 6971–7015, 2015

Evaluating the Community Land Model in a pine stand

J. Mao et al.

Title Page

Abstract	Introduction
Conclusions	References
Tables	Figures

◄ | ►|
◄ | ►
Back | Close

Full Screen / Esc

Printer-friendly Version

Interactive Discussion

Abstract

Carbon allocation and flow through ecosystems regulate land surface–atmosphere CO_2 exchange and thus is a key, albeit uncertain, component of mechanistic models. The Partitioning in Trees and Soil (PiTS) experiment-model project tracked carbon allocation through a young *Pinus taeda* stand following pulse-labeling with $^{13}CO_2$ and two levels of shading. The field component of this project provided process-oriented data that was used to evaluate and improve terrestrial biosphere model simulations of rapid shifts in carbon allocation and hydrological dynamics under varying environmental conditions. Here we tested the performance of the Community Land Model version 4 (CLM4) in capturing short-term carbon and water dynamics in relation to manipulative shading treatments, and the timing and magnitude of carbon fluxes through various compartments of the ecosystem. For CLM4 to closely simulate pretreatment conditions, we calibrated select model parameters with pretreatment observational data. Compared to CLM4 simulations with default parameters, CLM4 with calibrated model parameters was able to better simulate pretreatment vegetation carbon pools, light response curves, and other initial states and fluxes of carbon and water. Over a 3 week treatment period, the calibrated CLM4 generally reproduced the impacts of shading on average soil moisture at 15–95 cm depth, transpiration, relative change in stem carbon, and soil C_{O_2} efflux rate, although some discrepancies in the estimation of magnitudes and temporal evolutions existed. CLM4, however, was not able to track the progression of the $^{13}CO_2$ label from the atmosphere through foliage, phloem, roots or surface soil CO_2 efflux, even when optimized model parameters were used. This model bias arises, in part, from the lack of a short-term non-structural carbohydrate storage pool and progressive timing of within-plant transport, thus indicating a need for future work to improve the allocation routines in CLM4. Overall, these types of detailed evaluations of CLM4, paired with intensive field manipulations, can help to identify model strengths and weaknesses, model uncertainties, and additional observations necessary for future model development.

1 Introduction

Accurate projection of the changing global climate, given a particular scenario of future greenhouse gas emissions or concentrations, is largely determined by adequate representation of mechanistic processes in Earth System Models (ESMs) (Taylor et al., 2012). Land Surface Models (LSMs) and their associated biogeophysical and biogeochemical parameterizations are key determinants of the ESMs' fidelity in characterization and quantification of the complex feedbacks in the Earth System (Arora et al., 2013; Friedlingstein et al., 2006; Pitman, 2003). Modeling groups have increasingly used observational data and mechanistic knowledge of processes to advance the development of LSMs (Best et al., 2011; Dai et al., 2003; Krinner et al., 2005; Oleson et al., 2013; Wang et al., 2011). Global and regional observations of land surface fluxes, states, and dynamic vegetation change offer insights into the large-scale interactions between the land surface and atmosphere, and hence facilitate model improvements at relevant scales in space and time (Beer et al., 2010; Huntzinger et al., 2012; Luo et al., 2012; Randerson et al., 2009). However, to better quantify and reduce uncertainties arising from deficiencies in model process representation, parameters, driver datasets and initial conditions, there has been significant effort to evaluate and to calibrate LSMs against site-scale observations and experimental manipulations (Baldocchi et al., 2001; De Kauwe et al., 2014; Hanson et al., 2004; Ostle et al., 2009; Raczka et al., 2013; Richardson et al., 2012; Schaefer et al., 2012; Schwalm et al., 2010; Stoy et al., 2013; Walker et al., 2014; Williams et al., 2009; Zaehle et al., 2014). Further, model development from these focused site-scale studies, especially in close collaboration with experimentalists, can potentially inform and prioritize new experiments and observations that are specifically designed to advance critical terrestrial ecosystems and processes (Shi et al., 2015).

The Community Land Model (CLM) is an advanced LSM with a comprehensive mechanistic parameterization of carbon (C), water, and energy budgets for diverse land types that can be applied across multiple temporal scales (Oleson et al., 2010, 2013). It

is traditionally evaluated against historical observations from a wide range of sources, and these evaluations have resulted in rapid progress toward better model performance and hence upgraded model versions (Bauerle et al., 2012; Bonan et al., 2011, 2012; Koven et al., 2013; Lawrence et al., 2011; Mao et al., 2012a, b, 2013; Oleson et al., 2008; Randerson et al., 2009; Riley et al., 2011; Shi et al., 2011, 2013, 2015; Thornton et al., 2007). Nevertheless, little attention has been paid to CLM's ability to replicate short-term manipulative experiments, which provide an avenue for exploring and validating model response to sudden, large changes in environmental drivers that control physiological and ecological responses (Amthor et al., 2001; Bonan et al., 2013). Combined model-experiment projects can focus efforts on specific mechanistic processes whose representation in the model may be neither adequate nor appropriate for specific sites (Walker et al., 2014; Zaehle et al., 2014). Extending these model-experiment evaluations and ensuing model refinements to additional sites of the same and different ecosystem types improves confidence in the regional and global scale adequacy of the LSM's mechanistic process representation and parameterization.

Photosynthetic C assimilation, the allocation of photosynthesis products into tissues with different turnover rates, and the respiration of C back into the atmosphere are important determinants of the CO_2 exchange between the terrestrial biosphere and the atmosphere (Schimel et al., 2001). Biosphere–atmosphere C exchange is dynamically mediated by weather, soil conditions, vegetation community composition and phenology, and natural and anthropogenic disturbances (Cannell and Dewar, 1994; Litton et al., 2007). Mechanistic characterization of the fate of photosynthetically-fixed C, in particular the magnitude and timing of C allocation among plant compartments, is a major challenge for experimental and modeling communities (Epron et al., 2012). Various C-allocation schemes have been proposed and implemented in LSMs to capture both the dynamic changes in C allocation and response to external conditions of C allocation (De Kauwe et al., 2014). They generally employ either fixed coefficients or in some cases dynamic coefficents that are functions of time or time-varying external conditions to allocate assimilated C to different plant components (e.g., leaves and stems). These

allocation schemes and coefficients are generally not well constrained by observations. More process-based understanding, better measurement techniques, and targeted experimental manipulations are needed to better constrain allocation within the model structure and the models' overall representations of C dynamics.

5   In this study, our specific goal was to test the representation of C uptake and allocation patterns of a site-scale, point version of CLM version (PTCLM) (Oleson et al., 2013) at an experimental field facility in Oak Ridge, Tennessee, USA. The "Partitioning in Trees and Soils" (PiTS) project exposed a young loblolly pine (*Pinus taeda*) stand to a pulse of air enriched with $^{13}CO_2$, then tracked that label from the foliage, through the

10   stem and roots and ultimately out of the soil as respiratory flux (Warren et al., 2012). Comprehensive ancillary data were collected both before and after the labeling treatment (Warren et al., 2013). In addition, over a three-week period, shade cloth was used to reduce incident solar radiation for some of the trees; one-half of the trees received moderate shading (68 % of ambient photosynthetically active radiation (PAR) passed

15   through the shade cloth), while the other half received heavy canopy shading (11 % of ambient PAR passed through the cloth). This experimental treatment was intended to provide data to test the model's allocation, growth and transpiration responses to short-term, abrupt changes in gross primary production (GPP), based on the assumption that the shading would substantially reduce the trees' photosynthetic assimilation.

20   Model evaluations are complicated by the concurrence of parametric and structural uncertainty, which confounds the attribution of model errors (Keenan et al., 2011). A model's performance might be off because of misrepresentation of mechanistic processes, poor parameterization of otherwise sound functional representations, or both. To minimize the influence of parametric uncertainty and focus on the ability of the CLM

25   model structure to reproduce the experimental treatment, we optimized selected CLM parameters against pre-treatment data. We then evaluated the performance of the calibrated CLM in the pre-treatment phase and again in the post-treatment phase without recalibration following simulation of the canopy shading and ^{13}CO treatments. Our intention is that by applying robust parameter optimization to the pre-treatment simu-

BGD

Evaluating the Community Land Model in a pine stand

J. Mao et al.

Title Page

Abstract | Introduction

Conclusions | References

Tables | Figures

|◄ | ►|

◄ | ►

Back | Close

Full Screen / Esc

Printer-friendly Version

Interactive Discussion

lations we will reduce parametric uncertainty (Fox et al., 2009; Ricciuto et al., 2011), leading to greater insight regarding model structural uncertainty in evaluation of the post-treatment results.

The manuscript is organized as follows: we first describe the observational data sets, the model, and the simulation design. We then present results comparing the model results with the field observations; we continue with a discussion of model limitations revealed by the simulations and implications for potential model improvement. We conclude with recommendations on designing future manipulative field experiments to further improve model performance.

2 Methodology

2.1 Experimental site description and observations

The project was conducted in a young loblolly pine stand at the University of Tennessee Forest Resources AgResearch and Education Center in Oak Ridge, Tennessee. The soil is classified as a silty-clay-loam (13.3 % sand; 35.7 % clay; 51.0 % silt), with bulk density ranging from 1.2 to 1.4 g cm^{-3} at 10 to 70 cm depth. One-year-old seedlings (1 g C m^{-2}, Griffin et al., 1995) were planted at 2.5 × 3 m spacing in 2003, and the experiment was conducted in 2010 when the trees were ∼ 7 m tall.

In 2010, a subset of eight of the trees, adjacent to one another, and their soils, were instrumented with automated sensors to continuously measure soil temperature, soil moisture vertically throughout the soil profile, soil surface $^{12}CO_2$ and $^{13}CO_2$ efflux, root production at 10 and 30 cm depths, stem sap flow, and stem diameter (Warren et al., 2012). Various measurements were manually collected periodically, including predawn foliar water potential, photosynthetic light- and CO_2-response curves, root biomass, growth, and mortality, and soil C and nutrient content. Meteorological data were collected every 30 min at 2 m height in an adjacent open field, and included wind speed, air temperature, photosynthetically active and shortwave radiation, precipitation, and

Full Screen / Esc

Printer-friendly Version

Interactive Discussion

relative humidity. Additionally, in order to assess conditions under the shade cloth treatments (described below), short-term measurements of wind speed, temperature, and humidity were collected at the canopy surface following shade cloth installation. Linear regressions between meteorological data from under the shade cloth and from the open field were used to estimate conditions at the canopy surface during the experimental period (Fig. 1a, b). Results indicate wind speed (u) was ∼ 45 % (±15 %; ±1 SD) lower, relative humidity (RH) was ∼ 6 % (±5 %; ±1 SD) greater, and temperature (T) was ∼ 0.11 °C (±0.82 °C; ±1 SD) lower under both levels of shading as compared with the adjacent open-field meteorological station.

Following several weeks of pre-treatment measurements, the eight study trees were enclosed with plastic film stretched over a frame surrounding the trees, and then trees were exposed to 53 L of 99 atom % $^{13}CO_2$ label for 45 min. The plastic was removed and replaced with light shade (LS) or heavy shade (HS) cloth, each of which covered four trees and provided differential levels of PAR at the canopy surface for 3 weeks following the labeling (e.g., Fig. 1c). Pre-treatment non-destructive measurements of soil moisture, soil temperature, soil respiration, sap flow and stem growth were made for several weeks prior to the labeling. For 3 weeks after the labelling and during the shading treatment, destructive measurements of foliage, stem phloem tissue, roots and soil were collected to assess presence of the ^{13}C label, and linked to concurrent automated measurements of $^{13}CO_2$ from the soil surface (Warren et al., 2012). Experimental results and additional details on the site and experimental design are in Warren et al. (2012) and datasets are available online (Warren et al., 2013).

2.2 Model description

We used CLM4 (Oleson et al., 2010), the land component of the Community Earth System Model (CESM) (Gent et al., 2011), to simulate the manipulated processes in the PiTS study. This CLM version includes fully prognostic carbon and nitrogen representations for its vegetation, litter, and soil biogeochemistry components (Oleson et al., 2010, 2013; Thornton and Rosenbloom, 2005; Thornton et al., 2007).

Carbon allocation in this version of CLM is simplistic. After maintenance respiration demands are calculated and subtracted from gross primary productivity (GPP), and after nitrogen downregulation of GPP is calculated, the remaining available carbon is allocated at each half-hourly time step following annually fixed ratios of leaf to stem and root carbon pools, and to resulting growth respiration. The allocation ratio between stem and leaf is a function of the previous year's net primary productivity (NPP), while all other allocation ratios are fixed throughout the simulation for a given plant functional type. For ^{13}C, photosynthetic fractionation is calculated and photosynthetically fixed ^{13}C is immediately allocated to plant pools following the above description. There is no further fractionation in within-plant processes or during decomposition (Oleson et al., 2013).

Several major developments of CLM performed specifically for this study include: (1) introducing the ability to represent the shade effect and experimental labeling by driving the model with observed atmospheric $^{13}CO_2$ concentrations, where before $^{13}CO_2$ was assumed to be constant fraction of CO_2, (2) improvement of the site-level simulation workflow and leveraging of the capability for single-point implementation of PTCLM, (3) calibration of the selected model parameters for the pre- and post-treatment periods with parameterization optimization techniques, and (4) adding functional unit test capability for the photosynthesis subroutines.

2.2.1 Description of PTCLM simulation

To perform simulations at the PiTS site, we used PTCLM, a scripting framework to run site-level simulations of CLM more efficiently than the full model and with a high degree of automation and the ability to use site-specific forcing and initialization data (Oleson et al., 2013). To initialize soil and vegetation carbon stocks, each PTCLM simulation included 600 years of accelerated decomposition spinup (Thornton and Rosenbloom, 2005), 1000 years of normal spinup, and a transient simulation between 1850–2010. Long-term meteorological driver data were not available at the PiTS site, and instead were taken from the nearby Walker Branch and Chestnut Ridge eddy covariance sites

Full Screen / Esc

Printer-friendly Version

Interactive Discussion

(Hanson et al., 2004) for the years 2000–2010. These input data were cycled continuously to drive the model through the spinup and transient simulations. We replaced the meteorology from the eddy covariance sites with observed data at the treatment sites starting at the beginning of the $^{13}CO_2$ treatment in September 2010 (Warren et al., 2012). Incoming longwave radiation, which is a required CLM input, was not measured. We assumed that the heavy shade cloth emitted downward longwave radiation at a blackbody temperature similar to that of the air temperature, and that the light shade cloth did not impact incoming longwave radiation significantly. In the light shade case, we therefore applied the model's internal estimate of incoming longwave radiation, which uses clear-sky assumptions about atmospheric temperature and emissivity (Idso, 1981). These assumptions were verified by later measurements of both the light and heavy shade cloths with an infrared camera (data not shown).

2.2.2 Model calibration for pre- and post-treatment periods

To evaluate the ability of CLM to simulate the response of the loblolly stand to the experimental treatments, we first calibrated the model to simulate the pretreatment conditions as closely as possible using observations and prior information about model parameters. For calibration data, we used biomass estimated from allometry, pretreatment $\delta^{13}C$ values in leaf and root carbon pools, sap flow, and soil respiration observations from the 20 days preceding the ^{13}CO labeling and shading treatments. Because CLM predicts canopy transpiration but not sap flow, daily transpiration during the experiment was estimated by scaling the sap flow measurements using sapwood area and ground area covered by the rooting system (Wullschleger et al., 2001; Warren et al., 2011). Here we assume the rooting system of each tree occupied $7.5\,m^2$ of ground area based on the spacing between the trees. For consistency purpose, the sap flow is hereafter called transpiration for both the observational and modeled results. Some model parameters were estimated directly from observations (Table 1). Other parameters for which more direct estimation was not possible were optimized to maximize fit between model results and the observed calibration data (Table 1). The selection of

parameters for optimization was based on formal sensitivity analysis (Sargsyan et al., 2013) and prior experience with the model. We defined the sum of squared errors (SSE) between simulation and observations weighted by data uncertainty as the cost function for the optimization. Next, we selected a calibration method using that cost function. Calibration of nonlinear models such as CLM using multiple observations can be problematic because of local optima in the cost function. To reduce this possibility, we used a genetic algorithm (Runarsson and Yao, 2000). Simulations were performed in parallel using 64 processors, each running one single-site simulation over 100 iterations for a total of 6400 model simulations. The parameter set that minimized the cost function was selected as the optimal solution. Note that this method does not estimate parameter uncertainty (i.e., probability distributions of parameter values), but estimates the set of singular parameter values that provides the best fit with observations.

For the pretreatment (pre-labeling) period, we compared the standard version of the model (PRE-STD) with the optimized version (PRE-OPT). The model with optimized parameters was used in simulations for the shading treatment period for both the high shade and low shade treatments. Because of uncertainties associated with simulated stomatal conductance and transpiration in high-shade conditions, we performed additional parameter calibrations for the parameters mp (slope of the Ball-Berry stomatal conductance formulation) and bp (intercept of the Ball-Berry stomatal conductance formulation) using the genetic algorithm optimization. However, these calibrations were performed separately using only transpiration and stem growth data during the treatment period (HS_MB), with results discussed below.

2.2.3 Evaluation of CLM photosynthesis functions

There is considerable value in evaluating fundamental processes in CLM, and other models, at more than one scale or level of system organization. Evaluating the model's representation of photosynthesis, for example, at both the leaf and whole canopy or stand level can provide insights into the model's scaling relationships (e.g., the integration of leaf photosynthesis through the canopy). However, limitations of the current

code structure make it tedious to examine the functional representation of processes in CLM at scales or levels below that of the stand/ecosystem/plant function type for which the model normally generates output. This is especially true if the evaluation requires multiple runs of the model under, for example, different environmental conditions, with alternative parameter values, or for optimization. Accordingly, Wang et al. (2014) have developed a functional unit testing platform allowing direct comparison between the output of functional processes simulated by CLM and the corresponding field observations. In brief, the functional unit testing isolates targeted CLM processes and functional units (e.g., subroutines) into standalone modules that can be run with specified environmental conditions and parameter values without executing the entire CLM framework. The platform then provides links with observational data against which the functional unit simulations can be evaluated. Further details can be found in Wang et al. (2014). Here we used the functional unit testing framework to evaluate CLM's representation of the photosynthetic light response at the scale of the individual leaf against light-response curves obtained by Warren et al. (2012) for foliage in the upper canopy of trees at the PiTS experimental site prior to the shade treatment.

3 Results

Mean surface air temperature adjacent to the site decreased from Day −20 to 4 ("negative" days refer to days prior to the addition of $^{13}CO_2$ and shading treatments), then recovered somewhat and remained without obvious trend but with variation for the rest of the post-labeling period (Day 5 to 25) (Fig. 2a). Peak $^{13}CO_2$ concentration occurred on Day 0 as a consequence of the short-term labeling event (Fig. 2b). The impact of the shading treatments (Day 0 to 25) on shortwave radiation was noticeable (Fig. 2b).

The model predicted exponential growth in all biomass pools was observed during the 8 years pre-treatment, with perhaps some slowing in the final year (Fig. 3a). Compared to the standard CLM results, C stocks of the simulation with optimized parameters were lower and closer to observation-based estimates of leaf, stem, root and

total aboveground biomass (Baldwin and Feduccia, 1987; Naidu et al., 1998; Vanlear et al., 1986). Before parameter optimization, the photosynthesis module of CLM overestimated observed net assimilation at the leaf level under moderate and high PAR conditions, which is consistent with the biomass being too high in that simulation. With optimization, assimilation was reduced, especially at PAR greater than approximately $250\,\mu mol\,m^{-2}\,s^{-1}$ (Fig. 3b). Optimization substantially improved agreement with observations at higher PAR, albeit with some loss of agreement at light levels below approximately $200\,\mu mol\,m^{-2}\,s^{-1}$ (PRE_OPT simulations, Fig. 3b). Overall, the CLM-simulated light-response curve using the PRE_OPT parameterization was in better agreement with the observed light-response curve. It should be noted that the improvement was realized with parameters optimized against stand-level observations (Sect. 2.2.2) and not the leaf-level observations of photosynthesis, which served as an independent validation of the optimized model. The persistently larger difference between simulated and observed assimilation at PAR of approximately $500\,\mu mol\,m^{-2}\,s^{-1}$ is a consequence of the assumption in CLM4 of carboxylation being limited by a single factor (i.e, the calculation of the limiting carboxylation rate as the absolute minimum value of the RuBisCO-, RuBP regeneration- and TPU-limited rates of carboxylation) (Harley and Sharkey, 1991). Assuming co-limitation between the individually limited rates of carboxylation, a smoother transition between limiting factors and an improved fit with observations at the transition point of approximately $500\,\mu mol\,m^{-2}\,s^{-1}$ can be obtained by solving for the minimum carboxylation rate using coupled quadratics as in Collatz et al. (1991).

Using parameters optimized against the pre-treatment data, soil temperature predicted by CLM at 0–5 cm depth had a consistent overestimation bias of 1–2 °C, but the model closely reproduced the daily variation and decreasing tendency in surface soil temperature in both the pre-treatment and post-treatment periods (Fig. 4a). No clear influence of shading treatments on this soil state variable was seen in either the observational data or model simulations. Substantial variability in observed soil moisture (integrated for 15–95 cm depth) was found among samples taken near different trees under the same shading treatment (Fig. 4b). Observed LS soil water was lower than

that of the HS soil water at the start of the treatment period, probably because of local differences in soil properties and pretreatment evapotranspiration. The difference between observed LS and HS soil water content increased during the treatment period, suggesting reduced evapotranspiration in the HS plots, as supported by observations of slightly reduced transpiration under HS relative to that under LS (Fig. 4c). Following precipitation events on Days 7, 10, and 15, both observed and simulated soil water content increased (compare Figs. 2a and 4b). CLM systematically overestimated the magnitude of soil water content by 6–8 % (units are volume % of water in soil). While CLM did not capture the initial difference between mean observed HS and LS soil moisture, the model captured the reduction in LS soil water during the treatment period compared to the HS treatment. Before the implementation of shade treatments, the trees assigned to HS were observed to have higher transpiration than the LS trees (Fig. 4c), likely a consequence of the higher biomass and leaf area of the HS trees (Warren et al., 2012) and perhaps also higher soil water content (Fig. 4b). We used the pretreatment transpiration data to calibrate CLM, and the model simulated the pretreatment observations well in terms of both magnitude and temporal variations (Fig. 4c). After the treatment initiation, decreased transpiration was seen in both observations and model simulations for the HS and LS trees. For the LS case, CLM captured the observed transpiration well. However in the HS case, CLM predicted a sharp reduction in transpiration, whereas the observations differ relatively little from the LS case. To investigate this difference further, we performed a second optimization for the Ball-Berry stomatal conductance slope and intercept terms (HS_MB). However, despite increasing these parameters to near the maximum acceptable values (Table 1), the HS_MB optimization fails to capture the measured transpiration.

In contrast with the continued increase of stem carbon in the observed LS trees, the stem carbon of the observed HS trees declined over the shading treatment period (Fig. 5a). The model captured that basic difference in the observed response of stem carbon to HS and LS, but overestimated the rate of change under LS and simulated an essential halt in growth under HS rather than the observed decline in growth.

The shorter-term (3–5 day) variation in stem carbon (based on diameter change) under shading (Fig. 5a) we attribute primarily to precipitation events and changing soil moisture (Figs. 2a and 4b), and the accompanying swelling and shrinkage of stem diameter, which translates through the allometric functions to apparent changes in stem biomass. Stem diameter can shrink or swell based on changes in stem xylem water content, bark water content, and cambial growth, and is dependent on xylem water potential, vapor pressure deficit, C availability, non-structural carbohydrate concentrations, and C allocation (Vandegehuchte et al., 2014). C allocation to stem growth is revealed by a step-wise increase in stem diameter that occurs in response to favorable conditions, and that is maintained under less favorable conditions. The LS treatment clearly displayed the step-wise increases in stem diameter, while the HS treatment displayed a reduction in stem diameter. The shrinking stem diameter of HS trees indicates a decline in xylem and phloem water content likely linked to phloem sugar concentration. The HS treatment certainly reduced foliar C uptake and C available for phloem loading and allocation to cambial growth (Warren et al., 2012). The model displayed almost no short-term variability in stem carbon – the model does not represent stem swelling and shrinking with water status.

Both observed and simulated soil respiration tended to decline over the study period (after Day −10 in the observations) (Fig. 5b). We attribute that decline to corresponding decreases in temperature and soil moisture (Fig. 4a, b). The tendency for that change in environmental conditions to slow or reverse itself between Day 5 to 10 (Fig. 4a, b), appears to be reflected in a slowing or halting of the decline in soil respiration, especially in the model but also in the observations (Fig. 5b). The pretreatment soil respiration beneath the trees chosen for the HS treatment was 30 % higher than under those selected for the LS treatment. After the application of the shade treatments, relative differences between the observed HS and LS soil respiration were reduced, but respiration from HS soil remained higher. In contrast, simulated soil respiration was slightly higher under LS, although the difference is quite small. The observed temporal variability in soil respiration under both HS and LS is not well simulated, especially

the increase following precipitation events. Neither CLM4's carbon allocation to roots nor its predicted root respiration is dependent on soil water conditions, while the observations suggest the possibility of increased root growth following precipitation with an associated increase in growth respiration. CLM4's heterotrophic contribution to soil respiration may also have too little sensitivity and the timing of soil respiration response to soil water variation may also be too simplistic.

The observed foliar δ^{13}C increased above pretreatment background values almost immediately on Day 0 (the day of labeling), with slightly higher initial values under LS, followed by an exponential decline such that δ^{13}C of LS and HS were similar by Day 8, and δ^{13}C of LS was lower than the HS by Day 20 (Fig. 6a). Because the shading did not take place until after the labeling, observed differences in foliar ^{13}C are caused only by differences in leaf structure, photosynthetic rates and discrimination between the LS and HS trees. The model produced nearly equal foliar uptake of δ^{13}C on Day 0 in the LS and HS treatments. Neither the HS nor LS simulations captured the magnitude of the immediate spike and subsequent decline seen in the observations; simulated foliar δ^{13}C increases but does not spike with the simulated enrichment remaining nearly steady throughout the treatment period. Simulated points reflect daily average values. The lower magnitude of the simulated Day 0 value compared to subsequent days, reflects the fact that labeling was initiated near midday and on Day 0 the model experienced both background and enriched ^{13}C concentrations. The model does capture the fact that LS δ^{13}C declines faster than the high shade δ^{13}C. In the simulation, this occurs in the LS case because of the dilution of the δ^{13}C pulse with new photosynthate allocated to the leaf carbon pool. In the HS case, shading sharply reduces GPP, and nearly all photosynthate is allocated to maintenance respiration rather than structural carbon pools.

The observed phloem δ^{13}C peaked by Day 2 for both levels of shading, with greater enrichment in HS (Fig. 6b). In contrast, the model exhibited essentially no increase in phloem (live stem C in the model) δ^{13}C under either shade treatment and little difference between LS and HS. In both simulations, phloem δ^{13}C changed little compared

to observations, through the shading period (Fig. 6b). As with leaf δ^{13}C, phloem δ^{13}C in the LS case declines faster than in the HS case, also likely representing a dilution effect in the simulation. However, the observations indicate an opposite effect for phloem δ^{13}C.

There was no consistent shade treatment effect in the observed δ^{13}C of bulk fine-root samples (Fig. 6c), although after a few days, bulk roots were enriched over background under both treatments. On Day 20, observed δ^{13}C values in the fine-root pool were still higher than the background δ^{13}C levels, especially in the LS treatment. The model overestimated the background bulk root δ^{13}C for the pretreatment period by 2‰. As with foliar and phloem δ^{13}C, after Day 1 bulk root δ^{13}C values remained nearly stable in the HS simulation and slightly declined in the LS simulation, again representing dilution by new photosynthate.

The simulated δ^{13}C efflux from soil increased immediately with peak values on the labeling day (Day 0) for both treatments (Fig. 6d). These model results are inconsistent with the observed peak δ^{13}C values occurring on Day 3 for LS and Day 4 for HS. Observed δ^{13}C of soil CO_2 efflux decreased exponentially after the peak under both treatments. The model, on the other hand, simulated decreases of δ^{13}C soil CO_2 efflux to near pre-treatment levels immediately following the peak values and under both treatments returned to background levels by Day 1. A slight rising trend in both the simulated HS and LS cases represents the turnover of labeled leaf and fine root litter.

4 Discussion

4.1 Pretreatment results

The optimized model significantly improved simulations of pre-treatment tree biomass and transpiration (Fig. 3a). This was as expected since we used those observations in our parameter optimization. Perhaps not so expected, calibration with these observations improved leaf-level performance. Optimized parameters (Table 1) controlling

stomatal conductance changed little from default values for the temperate evergreen needle-leaf plant functional type (PFT). The fine-root to leaf allocation ratio increased from 1.0 to 1.24, which is well within the range of reported values (White et al., 2000). The fraction of leaf nitrogen in RuBisCO was 70 % higher than the model default value, and while on the high end, is consistent with measurements of other loblolly pine trees (Tissue et al., 1995). The temperature sensitivity of maintenance respiration ($Q_{10\,mr}$) nearly doubled from the default value of 1.5 to 2.83. This is higher than most values in the literature but is consistent with the value of 2.71 reported by Hamilton et al. (2001) for loblolly pine, although this value only pertains to leaf respiration. This higher Q_{10} value is also more consistent with the leaf-level data.

The leaf-level light response data provided an important validation metric for our calibration, since they were not used in the optimization (Fig. 3b). We found that the parameters most consistent with the biomass, transpiration, soil respiration and δ^{13}C data were also consistent with these leaf-level data, which gives confidence in both the model's ability to simulate the shading effect, and the model's ability to scale leaf-level processes to the canopy.

In addition to the importance of optimized model parameters, we also found that the initial seedling biomass was very important for simulating pretreatment biomass in this young forest in an exponential growth phase. This finding reinforces the understanding that models like CLM can be very sensitive to initial conditions, especially in systems, which are not in approximate or quasi- steady state. When designing experiments with an eye towards close engagement with models and the comparison of model and experimental results, attention should be given to measurements of the model's initial conditions as part of the experimental pretreatment characterization.

4.2 Treatment results

Early simulations of the shading treatment (not shown) were naively forced with reduced incoming shortwave radiation without any adjustment to the longwave radiation. This resulted in vegetation temperatures that were lower than the observed air temper-

Full Screen / Esc

Printer-friendly Version

Interactive Discussion

atures, high leaf boundary layer relative humidity, and nearly zero transpiration. This model limitation inspired additional measurements of the shade cloth with an infrared camera, showing that the cloth emitted longwave IR with a blackbody temperature near the observed air temperature. Using a modified forcing for longwave radiation (Figs. 1

5 and 2), we produced more realistic simulations for the HS treatment. The shade cloth used for the LS treatment was found to have little impact on IR, thus the original forcing was used for this treatment.

The lack of large differences in soil moisture between the LS and HS simulations is likely due to a combination of error in model inputs and weaknesses in model struc-

10 ture. Specifying a single site-specific soil texture may not have captured spatial hetero-geneity in soil biophysical properties, and it has been noted that improvement in CLM process representation is needed to capture realistic site hydrology (Li et al., 2011). The small difference between shading treatments in the observations of soil moisture (note the scale in Fig. 4b), albeit larger than the simulated difference, may be due to

15 a measurement artifact. It is known that there was some overlap of LS and HS roots that could dampen the differences in soil water between treatments. This was amelio-rated in subsequent PiTS projects by trenching and lining the trench with plastic film to isolate the treatments. Moreover, the large variability in observations of soil water suggests that the small differences between treatments in mean soil water are likely

20 not significant.

The observed decrease in transpiration with shading (Fig. 4) is affected by the shade treatment's impact on shortwave and longwave radiation and a coincident reduction in air temperature (Fig. 2). This effect was reproduced well in CLM for the LS case. However, observations do not show a strong response of transpiration in the HS case

25 but the model transpiration is highly reduced (Fig. 4c). Assuming that carbon assimila-tion is strongly reduced in the HS case as shown in the leaf-level light response curve (Fig. 3b), this implies a strong reduction in water use efficiency, which is not captured by the Ball-Berry conductance model as implemented in CLM (De Kauwe et al., 2013; Oleson et al., 2010, 2013). The HS_MB optimization for stomatal slope and intercept

Title Page

Abstract | Introduction

Conclusions | References

Tables | Figures

◄ | ►

◄ | ►

Back | Close

Full Screen / Esc

Printer-friendly Version

Interactive Discussion

parameters has little effect on transpiration despite increasing these parameter values well beyond reasonable ranges (Table 1; red line in Fig. 4c). The failure of the model under these conditions suggests a possibility that there is a diurnal or circadian control on conductance that is decoupled from photosynthesis and not currently captured. Another possibility is that there exists a strong nonlinearity in the relationship between stomatal conductance and net photosynthesis, which has been observed at low light levels and strongly impacts estimated transpiration (Barnard and Bauerle, 2013). Errors in modeled leaf temperature and leaf boundary layer vapor pressure deficit may also contribute to the discrepancy with observations, indicating a need for expanded environmental measurements in future work. Conductance may have been maintained to some extent by vapor pressure differences between the foliage and the shade cloth – indeed, dew was observed on unshaded trees in early morning, yet not on the shaded trees, indicating a differential temperature gradient that was not modeled. The behavior of stomatal conductance under low light has important implications for the carbon and energy balance, and the choice of conductance models has a strong impact on future predictions in climate models (Damour et al., 2010). More experimental results are needed to evaluate the effects of low-light conditions on stomatal conductance and the accuracy of current model representations of these effects. There may also have been pretreatment differences between the LS and HS trees that our assumptions in translating from sap flow to transpiration did not capture. Attention to pretreatment characterization in subsequent experiments with this translation might reduce this uncertainty.

In contrast with observations, there was no difference in simulated HS and LS soil respiration prior to the shading (Fig. 5b). After examining the simulated respiration fluxes, we determined the lack of pretreatment difference in simulated soil respiration and the small increase in post-treatment simulated soil respiration under LS is mainly a consequence of the higher growth respiration from coarse and fine roots that results from higher GPP and allocation to these pools in the LS conditions. This phenomenon might also explain the smaller post-treatment difference between observed HS and

⏮ | ⏭

◀ | ▶

Back | Close

Full Screen / Esc

Printer-friendly Version

Interactive Discussion

LS soil respiration, with higher root respiration under LS narrowing the pretreatment difference between HS and LS soil respiration.

The model's carbon allocation to the stem may also be less sensitive to short-term variation in environmental conditions than whatever contribution to observed (allometrically defined) variations in stem biomass are a result of actual stem growth and respiration (Fig. 5a). The model bias towards too much growth, or too little decline in growth does indicate that the treatment of allocation is too simplistic in CLM. Seasonal patterns of allocation are known to occur (Epron et al., 2012), while the allocation scheme in CLM is quite simple, using annually invariant ratios to allocate available carbon to leaf, stem, fine-root and coarse-root pools. Capturing the correct patterns of allocation (both where to and from which plant compartments, and when) is crucial for accurately modeling carbon fluxes, pool sizes, and associated climate feedbacks (De Kauwe et al., 2014; Epron et al., 2012; Litton et al., 2007). It is clear from this study that additional work is needed to improve allocation routines in CLM.

CLM allocates newly-assimilated carbon to plant pools and to growth/maintenance respiration every half-hourly model time step, while lags of several days are observed in this study. The resulting gap between modeled and observed C allocation was particularly evident in the model simulation of immediate ^{13}C enrichment in autotrophic and heterotrophic C fluxes. It will be important in future work to implement a short-term non-structural carbohydrate storage pools and a representation of within-plant transport of these pools along with a more realistic allocation scheme to capture these lags, as well as interactions of C allocation with environmental driving conditions. Also, modeled soil CO_2 efflux was too high on the first day of labeling and too small afterwards. This high simulated efflux represents a pulse of growth and maintenance respiration from the coarse and fine root pools, which is the result of near instantaneous allocation of assimilated carbon. The model's allocation to roots and the root's utilization of that carbon needs attention.

4.3 Implications for future model development and experimental design

A closer connection between carbon cycle modeling and experimental design is needed to systematically target the largest model process uncertainties systematically and also to improve predictive understanding. Modeling can inform experimental design by indicating where the largest uncertainties exist, while new data from experiments can constrain model predictions or lead to the integration of previously unconsidered processes. Considering model needs as part of the experimental design process (e.g., necessary drivers, and even the units in which variables are reported) can greatly facilitate the use and increase the benefits of experimental data. At the same time, considering the ability to simulate real-world experiments is best done as part of the model design process.

There were some limitations of this first PiTS observational dataset that have implications for subsequent efforts. Future experiments in a dogwood stand will address several issues based on knowledge gained from the PiTS 1 model-experiment efforts, including physical separation of treatments. New, additional observations will include a collection of absolute destructive tree biomass (rather than estimates based on allometric relationships), seasonal photosynthetic A/Ci curves, assessment of mycorrhizal C flux, seasonal replicate manipulations, and improved meteorological measurements. These additional observational data are necessary for more detailed model evaluation and improvement of model routines of seasonal C and allocation patterns.

Our framework for functional unit testing provides for the isolation and evaluation of fundamental mechanisms and processes (functions and subroutines) in CLM or similar models. This ability makes it possible to compare model results with observations made during an experiment that would be very difficult, if near impossible, to do with even a site-scale implementation of a LSM such as PTCLM. These models quite reasonably focus on, and generate output for, aggregate whole-stand properties such as stand-scale net ecosystem exchange and evapotranspiration. However, many experimental observations are at finer scales involving individual components of the stand

or ecosystem (e.g., individual leaves). As used in this study, the functional unit testing allows for model evaluation at the empirically accessible scales of experimental field observations (Fig. 3b).

5   Conclusions

The point version of CLM4 was successfully implemented, calibrated and evaluated against carbon and hydrology observations from the PiTS experimental manipulations at the 7 year-old loblolly pine trees. Our results demonstrate the important role of CLM4 physiological parameters (e.g., Ball-Berry stomatal conductance slope and Ball-Berry stomatal conductance intercept), initial carbon states (e.g., seedling biomass), driver data (e.g., the incoming longwave radiation), and internal algorithms (e.g., the allocation routines) in determining the performance of water and C flux and dynamic C allocation simulation. These systematic process-based evaluations through intimate linkage between model and experiment facilitate the identification of the model limitations and uncertainties. While the model is able to capture the pretreatment biomass and leaf-level responses, it is not able to reproduce the observed patterns of allocation revealed by the ^{13}C labeling experiment. Model development efforts should focus on improving the timing and magnitude of allocation patterns. Furthermore, the model was not able to reproduce the observed high-shade treatment effects, which resulted in strongly reduced transpiration but only slightly reduced productivity. Finally, this short-term model-experiment synthesis helped to inform and prioritize new complementary long-term observations in a follow-on experiment, including seasonal carbon allocation and partition patterns and seasonal A/Ci curves, for future CLM evaluation, calibration and improvement.

Full Screen / Esc

Printer-friendly Version

Interactive Discussion

Disclaimer

This manuscript has been authored by UT-Battelle, LLC under Contract No. DE-AC05-00OR22725 with the US Department of Energy. The United States Government retains and the publisher, by accepting the article for publication, acknowledges that the United States Government retains a non-exclusive, paid-up, irrevocable, world-wide license to publish or reproduce the published form of this manuscript, or allow others to do so, for United States Government purposes. The Department of Energy will provide public access to these results of federally sponsored research in accordance with the DOE Public Access Plan (http://energy.gov/downloads/doe-public-access-plan).

References

Amthor, J. S., Chen, J. M., Clein, J. S., Frolking, S. E., Goulden, M. L., Grant, R. F., Kimball, J. S., King, A. W., McGuire, A. D., Nikolov, N. T., Potter, C. S., Wang, S., and Wofsy, S. C.: Boreal forest CO_2 exchange and evapotranspiration predicted by nine ecosystem process models: intermodel comparisons and relationships to field measurements, J. Geophys. Res.-Atmos., 106, 33623–33648, 2001. (FOUND!)

Arora, V. K., Boer, G. J., Friedlingstein, P., Eby, M., Jones, C. D., Christian, J. R., Bonan, G., Bopp, L., Brovkin, V., and Cadule, P.: Carbon–concentration and carbon–climate feedbacks in CMIP5 Earth system models, J. Climate, 26, 5289–5314, 2013.

Baldocchi, D., Falge, E., Gu, L., Olson, R., Hollinger, D., Running, S., Anthoni, P., Bernhofer, C., Davis, K., and Evans, R.: FLUXNET: a new tool to study the temporal and spatial variability of ecosystem-scale carbon dioxide, water vapor, and energy flux densities, B. Am. Meteorol. Soc., 82, 2415–2434, 2001.

Baldwin, V. C. and Feduccia, D. P.: Loblolly pine growth and yield prediction for managed west Gulf plantations, USDA For. Ser. Res. Pap., SO-236, US Department of Agriculture, Forest Service, Southern Forest Experiment Station, New Orleans, LA, 27 pp., 1987.

Barnard, D. M. and Bauerle, W. L.: The implications of minimum stomatal conductance on modeling water flux in forest canopies, J. Geophys. Res.-Biogeo., 118, 1322–1333, 2013. (FOUND!)

Bauerle, W. L., Oren, R., Way, D. A., Qian, S. S., Stoy, P. C., Thornton, P. E., Bowden, J. D., Hoffman, F. M., and Reynolds, R. F.:, Photoperiodic regulation of the seasonal pattern of photosynthetic capacity and the implications for carbon cycling, P. Natl. Acad. Sci. USA, 109, 8612–8617, 2012.

Beer, C., Reichstein, M., Tomerlleri, E., Ciais, P., Jung, M., Carvalhai, N., Rodenbeck, C., Arain, M. A., Baldocchi, D., Bonan, G. B., Bondeau, A., Cescatti, A., Lasslop, G., Lindroth, A., Lomas, M., Luyssaert, S., Margolis, H., Oleson, K. W., Roupsard, O., Veenendaal, E., Viovy, N., Williams, C., Woodward, F. I., and Papale, D.: Terrestrial gross carbon dioxide uptake: global distribution and covariation with climate, Science, 329, 834–838, 2010.

Best, M. J., Pryor, M., Clark, D. B., Rooney, G. G., Essery, R.L. H., Ménard, C. B., Edwards, J. M., Hendry, M. A., Porson, A., Gedney, N., Mercado, L. M., Sitch, S., Blyth, E., Boucher, O., Cox, P. M., Grimmond, C. S. B., and Harding, R. J.: The Joint UK Land Environment Simulator (JULES), model description – Part 1: Energy and water fluxes, Geosci. Model Dev., 4, 677–699, doi:10.5194/gmd-4-677-2011, 2011.

Bonan, G. B., Lawrence, P. J., Oleson, K. W., Levis, S., Jung, M., Reichstein, M., Lawrence, D. M., and Swenson, S. C.: Improving canopy processes in the Community Land Model version 4 (CLM4) using global flux fields empirically inferred from FLUXNET data, J. Geophys. Res.-Biogeo., 116, G02014, doi:10.1029/2010JG001593, 2011.

Bonan, G. B., Oleson, K. W., Fisher, R. A., Lasslop, G., and Reichstein, M.: Reconciling leaf physiological traits and canopy flux data: Use of the TRY and FLUXNET databases in the Community Land Model version 4, J. Geophys. Res.-Biogeo., 117, G02026, doi:10.1029/2011JG001913, 2012.

Bonan, G. B., Hartman, M. D., Parton, W. J., and Wieder, W. R.: Evaluating litter decomposition in earth system models with long-term litterbag experiments: an example using the Community Land Model version 4 (CLM4), Glob. Change Biol., 19, 957–974, 2013.

Cannell, M. G. R. and Dewar, R. C.: Carbon allocation in trees – a review of concepts for modeling, Adv. Ecol. Res., 25, 59–104, 1994.

Collatz, G. J., Ball, J. T., Grivet, C., and Berry, J. A.: Physiological and environmental-regulation of stomatal conductance, photosynthesis and transpiration – a model that includes a laminar boundary-layer, Agr. Forest Meteorol., 54, 107–136, 1991.

Dai, Y. J., Zeng, X. B., Dickinson, R. E., Baker, I., Bonan, G. B., Bosilovich, M. G., Denning, A. S., Dimeyer, P. A., Houser, P. A., Niu, G. Y., Oleson, K. W., Scholosser, C. A., and Yang, Z., L.: The common land model, B. Am. Meteorol. Soc., 84, 1013, doi:10.1175/BAMS-84-8-1013, 2003.

Damour, G., Simonneau, T., Cochard, H., and Urban, L.: An overview of models of stomatal conductance at the leaf level, Plant Cell Environ., 33, 1419–1438, 2010.

De Kauwe, M. G., Medlyn, B. E., Zaehle, S., Walker, A. P., Dietze, M. C., Hickler, T., Jain, A. K., Luo, Y. Q., Parton, W. J., Prentice, I. C., Smith, B., Thornton, P. E., Wang, S. S., Wang, Y. P., Warlind, D., Weng, E. S., Crous, K. Y., Ellsworth, D. S., Hanson, P. J., Seok Kim, H., Warren, J. M., Oren, R., and Norby, R. J.: Forest water use and water use efficiency at elevated CO_2: a model-data intercomparison at two contrasting temperate forest FACE sites, Glob. Change Biol., 19, 1759–1779, 2013.

De Kauwe, M. G., Medlyn, B. E., Zaehle, S., Walker, A. P., Dietze, M. C., Wang, Y. P., Luo, Y. Q., Jain, A. K., El-Masri, B., Hickler, T., Warlind, D., Weng, E. S., Parton, W. J., Thornton, P. E., Wang, S. S., Prentice, I. C., Asao, S., Smith, B., McCarthy, H. R., Iversen, C. M., Hanson, P. J., Warren, J. M., Oren, R., and Norby, R. J.: Where does the carbon go? A model–data intercomparison of vegetation carbon allocation and turnover processes at two temperate forest free-air CO_2 enrichment sites, New Phytol., 203, 883–899, 2014.

Epron, D., Bahn, M., Derrien, D., Lattanzi, F. A., Pumpanen, J., Gessler, A., Hogberg, P., Maillard, P., Dannoura, M., Gerant, D., and Buchmann, N.: Pulse-labelling trees to study carbon allocation dynamics: a review of methods, current knowledge and future prospects, Tree Physiol., 32, 776–798, 2012.

Fox, A., Williams, M., Richardson, A. D., Cameron, D., Gove, J. H., Quaife, T., Ricciuto, D., Reichstein, M., Tomelleri, E., Trudinger, C. M., and Van Wijk, M. T.: The REFLEX project: Comparing different algorithms and implementations for the inversion of a terrestrial ecosystem model against eddy covariance data, Agr. Forest Meteorol., 149, 1597–1615, 2009.

Friedlingstein, P., Cox, P., Betts, R., Bopp, L., Von Bloh, W., Brovkin, V., Cadule, P., Doney, S., Eby, M., Fung, I., Bala, G., John, J., Jones, C., Joos, F., Kato, T., Kawamiya, M., Knorr, W., Lindsay, K., Matthews, H. D., Raddatz, T., Rayner, P., Reick, C., Roeckner, E., Schnitzler, K. G., Schnur, R., Strassmann, K., Weaver, A. J., Yoshikawa, C., and Zeng, N.: Climate-carbon cycle feedback analysis: results from the (CMIP)-M-4 model intercomparison, J. Climate, 19, 3337–3353, 2006.

Gent, P. R., Danabasoglu, G., Donner, L. J., Holland, M. M., Hunke, E. C., Jayne, S. R., Lawrence, K. M., Neale, R. B., Rasch, P. J., Vertenstein, M., Worley, P. H., Yang, Z. L, and Zhang, M. H.: The Community Climate System Model Version 4, J. Climate, 24, 4973–4991, 2011.

5 Griffin, K. L., Winner, W. E., and Strain, B. R.: Growth and dry matter partitioning in loblolly and ponderosa pine seedlings in response to carbon and nitrogen availability, New Phytol., 129, 547–556, 1995.

Hamilton, J. G., Thomas, R. B., and Delucia, E. H.: Direct and indirect effects of elevated CO_2 on leaf respiration in a forest ecosystem, Plant Cell Environ., 24, 975–982, 2001.

10 Hanson, P. J., Amthor, J. S., Wullschleger, S. D., Wilson, K. B., Grant, R. F., Hartley, A., Hui, D., Hunt, E. R., Johnson, D. W., Kimball, J. S., King, A. W., Luo, Y., McNulty, S. G., Sun, G., Thornton, P. E., Wang, S., Williams, M., Baldocchi, D. D., and Cushman, R. M.: Oak forest carbon and water simulations: model intercomparisons and evaluations against independent data, Ecol. Monogr., 74, 443–489, 2004.

15 Harley, P. C. and Sharkey, T. D.: An improved model of C_3 photosynthesis at high CO_2 – reversed O^{-2} sensitivity explained by lack of glycerate reentry into the chloroplast, Photosynth. Res., 27, 169–178, 1991.

Huntzinger, D. N., Post, W. M., Wei, Y., Michalak, A. M., West, T. O., Jacobson, A. R., Baker, I. T., Chen, J. M, Davis, K. J., Hayes, D. J., Hoffman, F. M., Jain, A. K., Liu, S., McGuire, A. D.,
20 Neilson, R. P., Potter, C., Poulter, B., Price, D., Raczka, B. M., Tian, H. Q., Thornton, P. E., Tomelleri, E., Viovy, N., Xiao, J., Yuan, W., Zeng, N., Zhao, M., and Cook, R.: North American Carbon Program (NACP) regional interim synthesis: terrestrial biospheric model intercomparison, Ecol. Model., 232, 144–157, 2012.

Idso, S. B.: A set of equations for full spectrum and 8-mu-m to 14-mu-m and 10.5-mu-m to
25 12.5-mu-m thermal-radiation from cloudless skies, Water Resour. Res., 17, 295–304, 1981.

Keenan, T. F., Carbone, M. S., Reichstein, M., and Richardson, A. D.: The model-data fusion pitfall: assuming certainty in an uncertain world, Oecologia, 167, 587–597, 2011.

Koven, C. D., Riley, W. J., Subin, Z. M., Tang, J. Y., Torn, M. S., Collins, W. D., Bonan, G. B., Lawrence, D. M., and Swenson, S. C.: The effect of vertically resolved soil biogeochemistry
30 and alternate soil C and N models on C dynamics of CLM4, Biogeosciences, 10, 7109–7131, doi:10.5194/bg-10-7109-2013, 2013.

Krinner, G., Viovy, N., de Noblet-Ducoudre, N., Ogee, J., Polcher, J., Friedlingstein, P., Ciais, P., Sitch, S., and Prentice, I. C.: A dynamic global vegetation model for stud-

Evaluating the Community Land Model in a pine stand

J. Mao et al.

ies of the coupled atmosphere–biosphere system, Global Biogeochem. Cy., 19, GB1015, doi:10.1029/2003GB002199, 2005.

Lawrence, D. M., Oleson, K. W., Fanner, M. G., Thornton, P. E., Swenson, S. C., Lawrence, P. J., Zeng, X. B., Yang, Z. L., Levis, S., Sakaguchi, K., Bonan, G. B., and Slater, A. G.: Parameterization improvements and functional and structural advances in version 4 of the Community Land Model, J. Adv. Model Earth Sy., 3., M03001, doi:10.1029/2011MS000045, 2011.

Li, H. Y., Huang, M. Y., Wigmosta, M. S., Ke, Y. H., Coleman, A. M., Leung, L. R., Wang, A. H., and Ricciuto, D. M.: Evaluating runoff simulations from the Community Land Model 4.0 using observations from flux towers and a mountainous watershed, J. Geophys. Res.-Atmos., 116, D24120, doi:10.1029/2011JD016276, 2011.

Litton, C. M., Raich, J. W., and Ryan, M. G.: Carbon allocation in forest ecosystems, Glob. Change Biol., 13, 2089–2109, 2007.

Luo, Y. Q., Randerson, J. T., Abramowitz, G., Bacour, C., Blyth, E., Carvalhais, N., Ciais, P., Dalmonech, D., Fisher, J. B., Fisher, R., Friedlingstein, P., Hibbard, K., Hoffman, F., Huntzinger, D., Jones, C. D., Koven, C., Lawrence, D., Li, D. J., Mahecha, M., Niu, S. L., Norby, R., Piao, S. L., Qi, X., Peylin, P., Prentice, I. C., Riley, W., Reichstein, M., Schwalm, C., Wang, Y. P., Xia, J. Y., Zaehle, S., and Zhou, X. H.: A framework for benchmarking land models, Biogeosciences, 9, 3857–3874, doi:10.5194/bg-9-3857-2012, 2012.

Mao, J. F., Shi, X. Y., Thornton, P. E., Piao, S. L., and Wang, X. H.: Causes of spring vegetation growth trends in the northern mid-high latitudes from 1982 to 2004, Environ. Res. Lett., 7, 014010, doi:10.1088/1748-9326/7/1/014010, 2012a.

Mao, J. F., Thornton, P. E., Shi, X. Y., Zhao, M. S., and Post, W. M.: Remote sensing evaluation of CLM4 GPP for the period 2000–09, J. Climate, 25, 5327–5342, 2012b.

Mao, J. F., Shi, X. Y., Thornton, P. E., Hoffman, F. M., Zhu, Z. C., and Myneni, R. B.: Global latitudinal-asymmetric vegetation growth trends and their driving mechanisms: 1982–2009, Remote Sens.-Basel, 5, 1484–1497, 2013.

Naidu, S. L., DeLucia, E. H., and Thomas, R. B.: Contrasting patterns of biomass allocation in dominant and suppressed loblolly pine, Can. J. Forest Res., 28, 1116–1124, 1998.

Oleson, K., Lawrence, D. M., Bonan, G. B., Drewniak, B., Huang, M., Koven, C. D., Levis, S., Li, F., Riley, W. J., Subin, Z. M., Swenson, S., Thornton, P. E., Bozbiyik, A., Fisher, R., Heald, C. L., Kluzek, E., Lamarque, J.-F., Lawrence, P. J., Leung, L. R., Lipscomb, W., Muszala, S. P., Ricciuto, D. M., Sacks, W. J., Sun, Y., Tang, J., and Yang, Z.-L.: Technical description of version 4.5 of the Community Land Model (CLM), NCAR Technical Note

NCAR/TN-503+STR, The National Center for Atmospheric Research (NCAR), Boulder, CO, USA, 420 pp., 2013.

Oleson, K. W., Niu, G.-Y., Yang, Z.-L., Lawrence, D. M., Thornton, P. E., Lawrence, P. J., Stoeckli, R., Dickinson, R. E., Bonan, G. B., Levis, S., Dai, A., and Qian, T.: Improvements to the Community Land Model and their impact on the hydrological cycle, J. Geophys. Res.-Biogeo., 113, G01021, doi:10.1029/2007JG000563, 2008.

Oleson, K. W., Lawrence, D. M., Gordon, B., Flanner, M. G., Kluzek, E., Lawrence, P. J., Levis, S., Swenson, S. C., Thornton, P. E., Dai, A., Decker, M., Dickinson, R., Feddema, J., Heald, C. L., Hoffman, F., Lamarque, J.-F., Mahowald, N., Niu, G.-Y., Qian, T., Randerson, J., Running, S., Sakaguchi, K., Slater, A., Stoeckli, R., Wang, A, Yang, Z.-L., Zeng, X. D., and Zeng, X. B.: Technical description of version 4.0 of the Community Land Model (CLM), NCAR Technical Note NCAR/TN 478+STR; The National Center for Atmospheric Research (NCAR), Boulder, CO, USA, 257 pp., 2010.

Ostle, N. J., Smith, P., Fisher, R., Woodward, F. I., Fisher, J. B., Smith, J. U., Galbraith, D., Levy, P., Meir, P., McNamar, N. P., and Bardgett, R. D.: Integrating plant-soil interactions into global carbon cycle models, J. Ecol., 97, 851–863, 2009.

Pitman, A. J.: The evolution of, and revolution in, land surface schemes designed for climate models, Int. J. Climatol., 23, 479–510, 2003.

Raczka, B. M., Davis, K. J., Huntzinger, D., Neilson, R. P., Poulter, B., Richardson, A. D., Xiao, J. F., Baker, I., Ciais, P., Keenan, T. F., Law, B., Post, W. M., Ricciuto, D., Schaefer, K., Tian, H. Q., Tomelleri, E., Verbeeck, H., and Viovy, N.:. Evaluation of continental carbon cycle simulations with North American flux tower observations, Ecol. Monogr., 83., 531–556, 2013.

Randerson, J. T., Hoffman, F. M., Thornton, P. E., Mahowald, N. M., Lindsay, K., Lee, Y. H., Nevison, C. D., Doney, S. C., Bonan, G., Stoeckli, R., Covey, C., Running, S. W., and Fung, I. Y.: Systematic assessment of terrestrial biogeochemistry in coupled climate-carbon models, Glob. Change Biol., 15, 2462–2484, 2009.

Ricciuto, D. M., King, A. W., Dragoni, D., and Post, W. M.: Parameter and prediction uncertainty in an optimized terrestrial carbon cycle model: effects of constraining variables and data record length, J. Geophys. Res.-Biogeo., 116, G01033, doi:10.1029/2010JG001400, 2011.

Richardson, A. D., Anderson, R. S., Arain, M. A., Barr, A. G., Bohrer, G., Chen, G. S., Chen, J. M., Ciais, P., Davis, K. J., Desai, A. R., Dietze, M. C., Dragoni, D., Garrity, S. R., Gough, C. M., Grant, R., Hollinger, D. Y., Margolis, H. A., McCaughey, H., Migliavacca, M.,

Title Page

Abstract | Introduction

Conclusions | References

Tables | Figures

◄ | ►

◄ | ►

Back | Close

Full Screen / Esc

Printer-friendly Version

Interactive Discussion

Monson, R. K., Munger, J. W., Poulter, B., Raczka, B. M., Ricciuto, D. M., Sahoo, A. K., Schaefer, K., Tian, H. Q., Vargas, R., Verbeeck, H., Xiao, J. F., and Xue, Y. K.: Terrestrial biosphere models need better representation of vegetation phenology: results from the North American Carbon Program Site Synthesis, Glob. Change Biol., 18, 566–584, 2012.

Riley, W. J., Subin, Z. M., Lawrence, D. M., Swenson, S. C., Torn, M. S., Meng, L., Mahowald, N. M., and Hess, P.: Barriers to predicting changes in global terrestrial methane fluxes: analyses using CLM4Me, a methane biogeochemistry model integrated in CESM, Biogeosciences, 8, 1925–1953, doi:10.5194/bg-8-1925-2011, 2011.

Runarsson, T. P. and Yao, X.: Stochastic ranking for constrained evolutionary optimization, IEEE T. Evolut. Comput., 4., 284–294, 2000.

Sargsyan, K., Safta, C., Habib, N. N., Debusschere, B. J., Ricciuto, D., and Thornton, P. E.: Dimensionality reduction for complex models via bayesian compressive sensing, Int. J. Uncertain. Quant., 4, 63–93, 2013. (NOT FOUND!)

Schaefer, K., Schwalm, C. R., Williams, C., Arain, M. A., Barr, A., Chen, J. M., Davis, K. J., Dimitrov, D., Hilton, T. W., Hollinger, D. Y., Humphreys, E., Poulter, B., Raczka, B. M., Richardson, A. D., Sahoo, A., Thornton, P. E., Vargas, R., Verbeeck, H., Anderson, R., Baker, I., Black, T. A., Bolstad, P., Chen, J. Q., Curtis, P. S., Desai, A. R., Dietze, M., Dragoni, D., Gough, C., Grant, R. F., Gu, L. H., Jain, A., Kucharik, C., Law, B., Liu, S. G., Lokipitiya, E., Margolis, H. A., Matamala, R., McCaughey, J. H., Monson, R., Munger, J. W., Oechel, W., Peng, C. H., Price, D. T., Ricciuto, D., Riley, W. J., Roulet, N., Tian, H. Q. Tonitto, C., Torn, M., Weng, E. S., and Zhou, X. L.: A model-data comparison of gross primary productivity: results from the North American Carbon Program site synthesis, J. Geophys. Res.-Biogeo., 117, G03010, doi:10.1029/2012JG001960, 2012.

Schimel, D. S., House, J. I., Hibbard, K. A., Bousquet, P., Ciais, P., Peylin, P., Braswell, B. H., Apps, M. J., Baker, D., Bondeau, A., Canadell, J., Churkina, G., Cramer, W., Denning, A. S., Field, C. B. Friendlingstein, P., Goodale, C., Heimann, M., Houghton, R. A., Melillo, J. M., Moore, B., Murdiyarso, D., Noble, I., Pacala, S. W., Prentice, I. C., Raupach, M. R., Rayner, P. J., Scholes, R. J., Steffen, W. L., and Wirth, C.: Recent patterns and mechanisms of carbon exchange by terrestrial ecosystems, Nature, 414, 169–172, 2001.

Schwalm, C. R., Williams, C. A., Schaefer, K., Anderson, R., Arain, M. A., Baker, I., Barr, A., Black, T. A., Chen, G. S., Chen, J. M., Ciais, P., Davis, K. J., Desai, A., Dietze, M., Dragoni, D., Fischer, M. L., Flanagan, L. B., Grant, R., Gu, L. H., Hollinger, D., Izaurralde, R. C., Kucharik, C., Lafleur, P., Law, B. E., Li, L. H., Li, Z. P., Liu, S. G., Lokupitiya, E., Luo, Y. Q.,

Evaluating the Community Land Model in a pine stand

J. Mao et al.

Ma, S. Y., Margolis, H., Matamala, R., McCaughey, H., Monson, R. K., Oechel, W. C., Peng, C. H., Poulter, B., Price, D. T., Ricciuto, D. M., Riley, W., Sahoo, A. K., Sprintsin, M., Sun, J. F., Tian, H. Q., Tonitto, C., Verbeeck, H., and Verma, S. B.: A model-data intercomparison of CO_2 exchange across North America: results from the North American Carbon Program site synthesis, J. Geophys. Res.-Biogeo., 115, G00H05, doi:10.1029/2009JG001229, 2010.

Shi, X., Mao, J., Thornton, P. E., Hoffman, F. M., and Post, W. M.: The impact of climate, CO_2, nitrogen deposition and land use change on simulated contemporary global river flow, Geophys. Res. Lett., 38, L08704, doi:10.1029/2011GL046773, 2011.

Shi, X. Y., Mao, J. F., Thornton, P. E., and Huang, M. Y.: Spatiotemporal patterns of evapotranspiration in response to multiple environmental factors simulated by the Community Land Model, Environ. Res. Lett., 8, 024012, doi:10.1088/1748-9326/8/2/024012, 2013.

Shi, X., Thornton, P. E., Ricciuto, D. M., Hanson, P. J., Mao, J., Sebestyen, S. D., Griffiths, N. A., and Bisht, G.: Representing northern peatland microtopography and hydrology within the Community Land Model, Biogeosciences Discuss., 12, 3381–3418, doi:10.5194/bgd-12-3381-2015, 2015.

Stoy, P. C., Dietze, M. C., Richardson, A. D., Vargas, R., Barr, A. G., Anderson, R. S., Arain, M. A., Baker, I. T., Black, T. A., Chen, J. M., Cook, R. B., Gough, C. M., Grant, R. F., Hollinger, D. Y., Izaurralde, R. C., Kucharik, C. J., Lafleur, P., Law, B. E., Liu, S., Lokupitiya, E., Luo, Y., Munger, J. W., Peng, C., Poulter, B., Price, D. T., Ricciuto, D. M., Riley, W. J., Sahoo, A. K., Schaefer, K., Schwalm, C. R., Tian, H., Verbeeck, H., and Weng, E.: Evaluating the agreement between measurements and models of net ecosystem exchange at different times and timescales using wavelet coherence: an example using data from the North American Carbon Program Site-Level Interim Synthesis, Biogeosciences, 10, 6893–6909, doi:10.5194/bg-10-6893-2013, 2013.

Taylor, K. E., Stouffer, R. J., and Meehl, G. A.: An overview of CMIP5 and the experiment design, B. Am. Meteorol. Soc., 93, 485–498, 2012.

Tissue, D. T., Thomas, R. B., and Strain, B. R.: Growth and photosynthesis of loblolly pine (*Pinus taeda*) after exposure to elevated CO_2 for 19 months in the field, Tree Physiol., 16, 49–59, 1995.

Thornton, P. E. and Rosenbloom, N. A.: Ecosystem model spin-up: Estimating steady state conditions in a coupled terrestrial carbon and nitrogen cycle model, Ecol. Model., 189, 25–48, 2005.

Thornton, P. E., Lamarque, J. F., Rosenbloom, N. A., and Mahowald, N. M.: Influence of carbon-nitrogen cycle coupling on land model response to CO_2 fertilization and climate variability, Global Biogeochem. Cy., 21, GB4018, doi:10.1029/2006GB002868, 2007.

Vandegehuchte, M. W., Guyot, A., Hubeau, M., De Swaef, T., Lockington, D. A., and Steppe, K.: Modelling reveals endogenous osmotic adaptation of storage tissue water potential as an important driver determining different stem diameter variation patterns in the mangrove species *Avicennia marina* and *Rhizophora stylosa*, Ann. Bot.-London, 114, 667–676, doi:10.1093/aob/mct311, 2014.

Vanlear, D. H., Taras, M. A., Waide, J. B., and Augspurger, M. K.: Comparison of biomass equations for planted vs. natural loblolly-pine stands of sawtimber size, Forest Ecol. Manag., 14, 205–210, 1986.

Walker, A. P., Hanson, P. J., De Kauwe, M. G., Medlyn, B. E., Zaehle, S., Asao, S., Dietze, M., Hickler, T., Huntingford, C., Iversen, C. M., Jain, A., Lomas, M., Luo, Y., McCarthy, H., Parton, W. J., Prentice, I. C., Thornton, P. E., Wang, S., Wang, Y.-P., Warlind, D., Weng, E., Warren, J. M., Woodward, F. I., Oren, R., and Norby, R. J.: Comprehensive ecosystem model-data synthesis using multiple data sets at two temperate forest free-air CO_2 enrichment experiments: model performance at ambient CO_2 concentration, J. Geophys. Res.-Biogeo., 119, 937–964, 2014.

Wang, D. L., Xu, Y., Thornton, P. E., King, A., Steed, C., Gu, L. H., and Schuchart, J.: A functional test platform for the Community Land Model, Environ. Modell. Softw., 55, 25–31, 2014.

Wang, Y. P., Kowalczyk, E., Leuning, R., Abramowitz, G., Raupach, M. R., Pak, B., van Gorsel, E., and Luhar, A.: Diagnosing errors in a land surface model (CABLE) in the time and frequency domains, J. Geophys. Res.-Biogeo., 116, G01034, doi:10.1029/2010JG001385, 2011.

Warren, J. M., Norby, R. J., and Wullschleger, S. D.: Elevated CO_2 enhances leaf senescence during extreme drought in a temperate forest, Tree Physiol., 31, 117–130, 2011.

Warren, J. M., Iversen, C. M., Garten, C. T., Norby, R. J., Childs, J., Brice, D., Evans, R. M., Gu, L., Thornton, P. E., and Weston, D. J.: Timing and magnitude of C partitioning through a young loblolly pine (*Pinus taeda* L.) stand using C-13 labeling and shade treatments, Tree Physiol., 32, 799–813, 2012.

Warren, J. M., Iversen, C. M., Garten Jr., C. T., Norby, R. J., Childs, J., Brice, D., Evans, R. M., Gu, L., Thornton, P. E., and Weston, D. J.: PiTS-1: Carbon partitioning in loblolly pine after ^{13}C labeling and shade treatments, Carbon Dioxide Information Analysis Center,

Evaluating the Community Land Model in a pine stand

J. Mao et al.

Oak Ridge National Laboratory, US Department of Energy, Oak Ridge, Tennessee, USA, doi:10.3334/CDIAC/ornlsfa.001, 2013.

White, M. A., Thornton, P. E., Running, S. W., and Nemani, R. R.: Parameterization and sensitivity analysis of the BIOME-BGC terrestrial ecosystem model: net primary production controls, Earth Interact., 4, 1–85, 2000.

Williams, M., Richardson, A. D., Reichstein, M., Stoy, P. C., Peylin, P., Verbeeck, H., Carvalhais, N., Jung, M., Hollinger, D. Y., Kattge, J., Leuning, R., Luo, Y., Tomelleri, E., Trudinger, C. M., and Wang, Y. -P.: Improving land surface models with FLUXNET data, Biogeosciences, 6, 1341–1359, doi:10.5194/bg-6-1341-2009, 2009.

Wullschleger, S. D., Hanson, P. J., and Todd, D. E.: Transpiration from a multi-species deciduous forest as estimated by xylem sap flow techniques, Forest Ecol. Manag., 143, 205–213, 2001.

Zaehle, S., Medlyn, B. E., De Kauwe, M. G., Walker, A. P., Dietze, M. C., Hickler, T., Luo, Y. Q., Wang, Y. P., El-Masri, B., Thornton, P., Jain, A., Wang, S. S., Warlind, D., Weng, W. S., Parton, W., Iversen, C. M., Gallet-Budynek, A., McCarthy, H., Finzi, A. C., Hanson, P. J., Prentice, I. C., Oren, R., and Norby, R. J.: Evaluation of 11 terrestrial carbon-nitrogen cycle models against observations from two temperate free-air CO_2 enrichment studies, New Phytol., 202, 803–822, 2014.

Table 1. Default PFT-level, site-specific and optimized parameters for the PiTS site used in CLM 4. PFT-level parameters are for the temperate evergreen needleleaf forest type. Optimized values were obtained using the pre-treatment data (PRE_OPT), and for the transpiration data during the shading period (HS_MB). In the HS_MB optimization, only the mp and bp parameters were optimized, while other parameters retain their pre-treatment optimization values.

Parameter	Description	Units	ENFT default	PRE_OPT	HS_MB
Measured					
slatop	Top of canopy specific leaf area	$m^2/g\,C$	1.00×10^{-2}	1.02×10^{-2}	1.02×10^{-2}
dsladlai	Change in SLA through per unit LAI	$g\,C^{-1}$	1.25×10^{-3}	0	0
leafcn	leaf C : N ratio	$g\,C/g\,N$	35	50	50
Optimized					
mp	Ball-Berry stomatal conductance slope	none	6	5.59	71.3
bp	Ball-Berry stomatal conductance intercept	$\mu mol\,m^{-2}\,s^{-1}$	5000	4960	61 100
froot_leaf	fine root to leaf allocation ratio	none	1	1.24	1.24
stem_leaf	stem to leaf allocation ratio	none	2.2[*]	3.29	3.29
flnr	fraction of leaf N in RuBisCO	none	0.05	0.0845	0.0845
q10_mr	maintenance respiration t sensitivity	none	1.5	2.83	2.83

[*] Stem-leaf allocation is a function of annual NPP. 2.2 is the nominal value at NPP = $800\,g\,C\,m^{-2}\,yr^{-1}$.
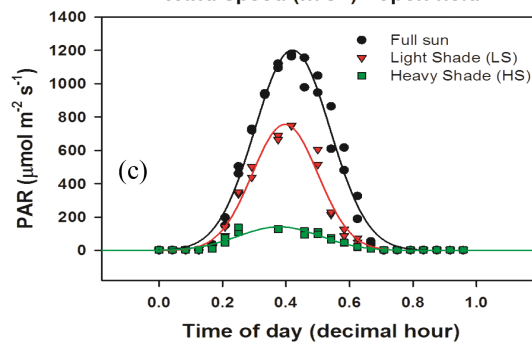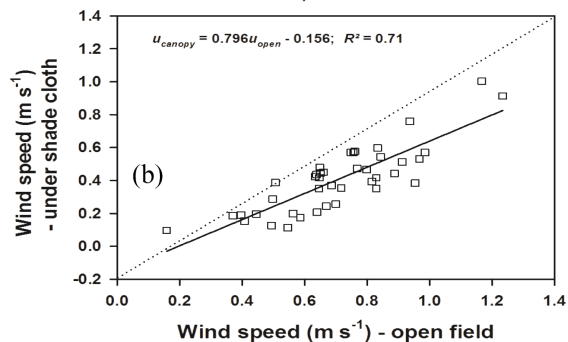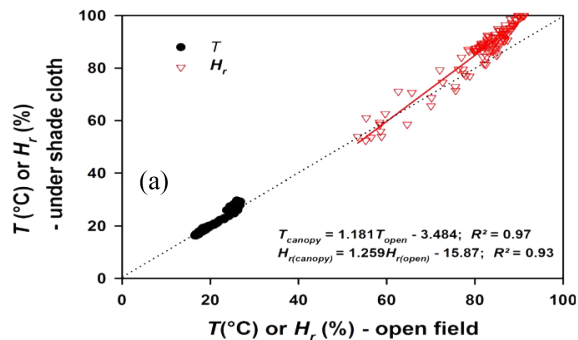
Figure 1. (a) Air temperature (T, ˚C), relative humidity (RH, %) and **(b)** wind speed (u, m s^{-1}) under the shade cloth at the top of the canopy compared with open field measurements at 2 m height; **(c)** typical diurnal patterns of photosynthetically active radiation (PAR, μmol m^{-2} s^{-1}) at the site under full sun, light shade or heavy shade treatments.
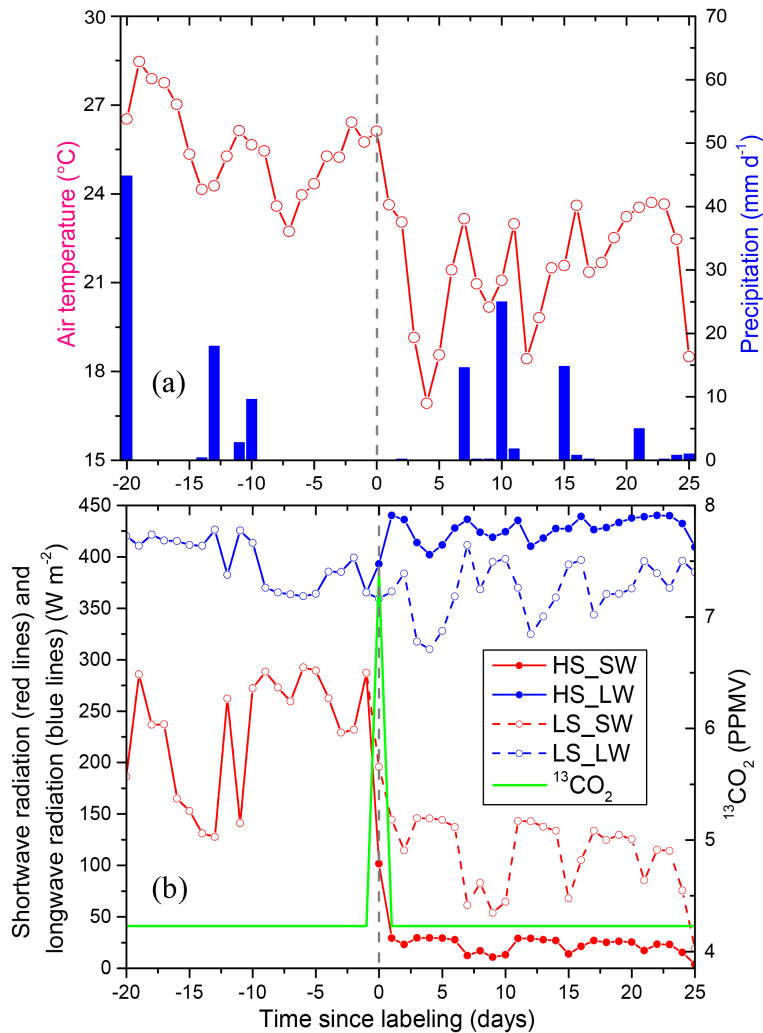
Figure 2. (a) Daily air temperature (°C) and precipitation (mm d^{-1}) for the pretreatment and treatment of light shade (LS) and heavy shade (HS) (Day −20 to 25), **(b)** change in atmospheric long wave radiation (LW, W m^{-2}), short wave radiation (SW, W m^{-2}) and $^{13}CO_2$ (PPMV) prior to and after exposure to shade treatments. Dashed gray line represents the starting day of the treatment.
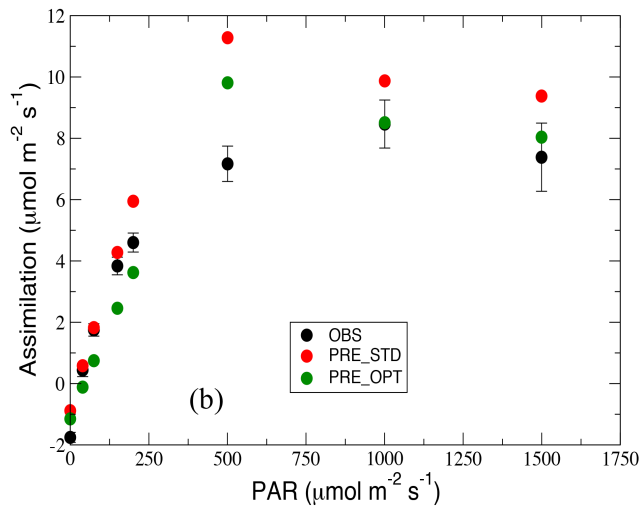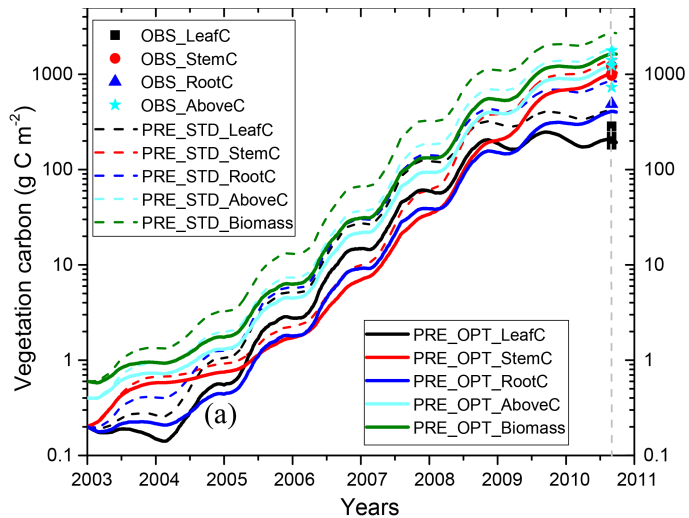
Full Screen / Esc

Printer-friendly Version

Interactive Discussion

Figure 3. (a) CLM simulated change of leaf carbon (PRE_STD_LeafC), stem carbon (PRE_STD_StemC), root carbon (PRE_STD_RootC), total above ground carbon (PRE_STD_AboveC) and total biomass (PRE_STD_Biomass) with default parameters, and change of those (PRE_OPT_LeafC, PRE_OPT_StemC, PRE_OPT_RootC, PRE_OPT_AboveC and PRE_OPT_Biomass) simulated with optimized parameters for the pretreatment period between year 2003 and 1 September (dashed gray line) of year 2010. Observational estimations of leaf (OBS_LeafC), stem (OBS_StemC), root (OBS_RootC) and aboveground carbon (OBS_AboveC) are based on measured stem diameters at breast height and allometric relationships from similarly aged loblolly pine (Baldwin, 1987; Naidu et al., 1998; Vanlear et al., 1986). Note that y axis is log-scaled. **(b)** Comparison of observed and simulated light response of top of the canopy leaves of loblolly pine at the PiTS-1 site. Solid black circles are mean ±1 SD of observations. Solid red and green circles are simulated results from the net photosynthesis module of the functional unit testing framework using site-observed parameters (PRE_STD) and optimized parameters (PRE_OPT), respectively (see Sect. 2.2.2). Simulations are with the mean observed internal CO_2 concentrations (C_i) and leaf temperatures (T_{leaf}) at the observed light (PAR) levels and the site's observed leaf nitrogen (Na).

Figure 4. (a) Observed (OBS) and CLM simulated daily soil temperature at 0–5 cm depth, **(b)** mean soil water content at 15–95 cm depth and **(c)** the transpiration before and after initiation of light shade (LS) or heavy shade (HS) treatments. MB represents the CLM simulation with optimized leaf conductance parameters. Dashed gray line in all the figures represents the starting day of the treatment. The error bars in **(b)** represent the SD of the observed soil water content.
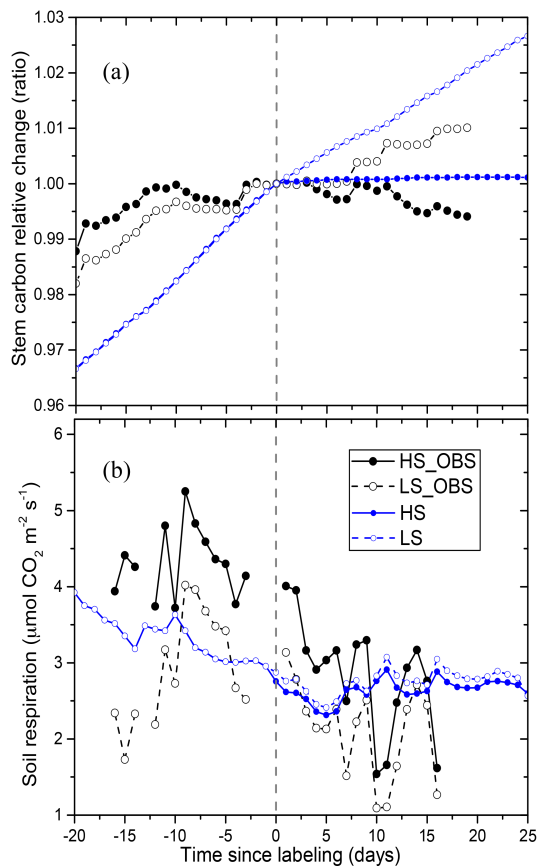
Full Screen / Esc

Printer-friendly Version

Interactive Discussion

Figure 5. (a) Observed (OBS) and CLM simulated daily stem carbon relative to Day 0, and **(b)** soil respiration prior to and after exposure to light shade (LS) and heavy shade (HS) treatments. Both observed and simulated stem carbon were normalized to 1 at Day 0. The simulated soil respiration is the combination of autotrophic from roots and heterotrophic respiration from the decay of litter and soil organic matter. Dashed gray line represents the starting day of the treatment.

Figure 6. (a) Observed (black) and CLM simulated (blue) change in δ^{13}C of **(a)** leaf, **(b)** phloem, **(c)** bulk root and **(d)** soil surface efflux δ^{13}C for the light shade (LS, open circle) and heavy shade (HS, filled circle) pretreatment and treatment periods. The $^{13}CO_2$ labeling pulse was initiated on 1 September in year 2010 (Day 0). Dashed gray line represents the starting day (again Day 0) of the shading treatment. To better visualize the model results, in the upper right corner of each figure, we show the CLM simulated δ^{13}C values for the light shade (open circle) and heavy shade (filled circle) treatments from Day 1 to Day 25.